ELSEVIER

Physics of the Earth and Planetary Interiors 130 (2002) 195–208

PHYSICS OF THE EARTH AND PLANETARY INTERIORS

www.elsevier.com/locate/pepi

Probing mid-mantle heterogeneity using PKP coda waves

Michael A.H. Hedlin*, Peter M. Shearer[1]

Cecil H. and Ida M. Green Institute of Geophysics and Planetary Physics, Scripps Institution of Oceanography, University of California, San Diego, La Jolla, CA 92093-0225, USA

Received 13 April 2001; accepted 17 January 2002

Abstract

We investigate the utility of PKP coda waves for studying weak scattering from small-scale heterogeneity in the mid-mantle. Coda waves are potentially a useful probe of heterogeneity in the mid-mantle because they are not preferentially scattered near the CMB, as PKP precursors are, but are sensitive to scattering at all depths. PKP coda waves have not been used for this purpose historically because of interference with other late-arriving energy due to near-surface resonance and scattering. Any study of deep mantle scattering using coda waves requires the removal of near-surface effects from the data. We have analyzed 3624 recordings of PKP precursors and coda made by stations in the Incorporated Research Institutions for Seismology (IRIS) Global Seismographic Network (GSN). To study the range and time dependence of the scattered waves, we binned and stacked envelopes of the recordings. We have considered precursors that arrive within a 20 s window before PKP and coda waves in a 60 s window after PKP. The PKP scattered waves increase in amplitude rapidly with range as predicted by scattering theory. At ranges below ∼125°, we predict and observe essentially no scattered energy preceding PKP. Coda amplitudes at these ranges are independent of range and provide an estimate of energy due to near-surface effects that we can expect at all ranges. We use the average coda amplitude at ranges from 120 to 125° to correct coda amplitudes at other ranges. PKP coda waves show a strong dependence on time and range and are clearly influenced by scattering in the lower mantle. PKP coda waves, however, do not provide a tighter constraint on the vertical distribution of mantle heterogeneity than is provided by precursors. This is due, in part, to relatively large scatter in coda amplitudes as revealed by a resampling analysis. Modeling using Rayleigh–Born scattering theory and an exponential autocorrelation function shows that PKP coda amplitudes are not highly sensitive to the vertical distribution of heterogeneity in the mantle. To illustrate this we consider single-scattering in two extreme models of mantle heterogeneity. One allows heterogeneity just at the CMB; the other includes heterogeneity throughout the mantle. The amplitudes of precursors are tightly constrained by our stack and support our earlier conclusion that small-scale heterogeneity is uniformly distributed throughout the lower mantle. The best-fit model includes 8 km scale length heterogeneity with an rms velocity contrast throughout the mantle of 1%.

Keywords: Seismology; Scattering; Born approximation; PKP-waves

1. Introduction

Since the pioneering work of Haddon and Cleary in the early 1970s, the high-frequency energy that precedes the inner core phase PKP (df) has been known to result from scattering in the mantle (Haddon, 1972; Haddon and Cleary, 1974; Fig. 1). These scattered waves arrive free of interference from late-arriving

* Corresponding author. Tel.: +1-858-534-8773; fax: +1-858-822-3372.
E-mail addresses: hedlin@ucsd.edu (M.A.H. Hedlin), pshearer@ucsd.edu (P.M. Shearer).
[1] Tel.: +1-858-534-2260; fax: +1-858-822-3372.

0031-9201/02/$ – see front matter
PII: S0031-9201(02)00007-9

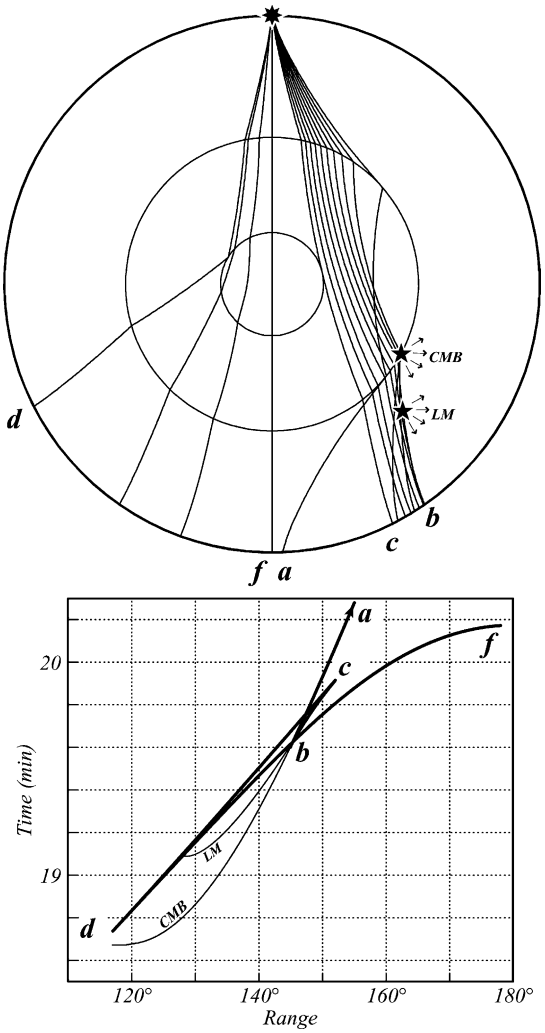

Fig. 1. Ray paths and travel times of the different branches of PKP for a source at the surface. The retrograde ab and prograde bc branches refract through the outer core. The cd branch is reflected from the inner core boundary. The df branch refracts through the inner core. Scattering involving the ab or bc branch can produce precursory arrivals as well as later arrivals that contribute to the d.f. coda. Scattering of d.f. will not cause d.f. precursors but will also contribute to the d.f. coda. Two hypothetical scatterers (labeled CMB and LM) produce precursors that can arrive no earlier than the labeled curves in the lower panel. The deepest scatterers will give rise to the earliest precursors. Although, we have depicted scattering from PKP to P near the receiver, precursors can also result from scattering from P to PKP on the source side.

near-surface scattered waves and thus provide a unique window into the small-scale structure of the deep earth. Numerous studies have used recordings of these precursors to investigate the physical properties of small-scale heterogeneity in the mantle (e.g. Cleary and Haddon, 1972; Doornbos and Husebye, 1972; Haddon and Cleary, 1974; King et al., 1974; Husebye et al., 1976; Doornbos, 1976, 1978; Bataille and Flatté, 1988; Cormier, 1995; Hedlin et al., 1995, 1997; Vidale and Hedlin, 1998; Shearer et al., 1998; Hedlin and Shearer, 2000; Wen, 2000). Although, a recent analysis by Hedlin et al. (1997) used GSN recordings of the precursors to study heterogeneity throughout the lower mantle, the geometry of the precursors favors studies of the deepest mantle as the preponderance of early arrivals come from great depth (Fig. 2). Relatively few precursors are due to scattering in the shallow mantle and these arrive at ranges very close to the b caustic and can be difficult to distinguish from PKP. Hedlin et al. (1997) modeled the weak scattering that gives rise to precursors using the Born approximation and found that the gradual growth of the precursors with time and range favored a model that included heterogeneity distributed with equal strength at all depths in the lower mantle. Models that include heterogeneity just at the CMB or within D″ produce early arrivals and thus sharper onsets than are seen in the data. This surprising result awaits confirmation by an independent analysis, as models involving multiple scattering near the CMB might also be able to explain the PKP precursor observations.

PKP coda waves are due largely to near surface scattering and resonance, but also include contributions from scattering throughout the mantle (Fig. 2). Evidence that lower mantle scattering contributes energy to PKP coda can be found in raw data in which recorded PKP coda amplitude variations with time and range mirror those observed in the precursors (Fig. 3). This basic observation suggests that we might be able to put tighter constraints on the strength of heterogeneity in the mantle using coda waves provided that we are able to correctly compensate coda amplitudes for near surface effects. It is this idea that we test in this paper. Although, there is evidence for lateral variations in mantle scattering intensity from PKP precursor studies (e.g. Hedlin and Shearer, 2000), we do not attempt to resolve such variations in the PKP coda. Rather, our goal is to obtain a basic understanding of

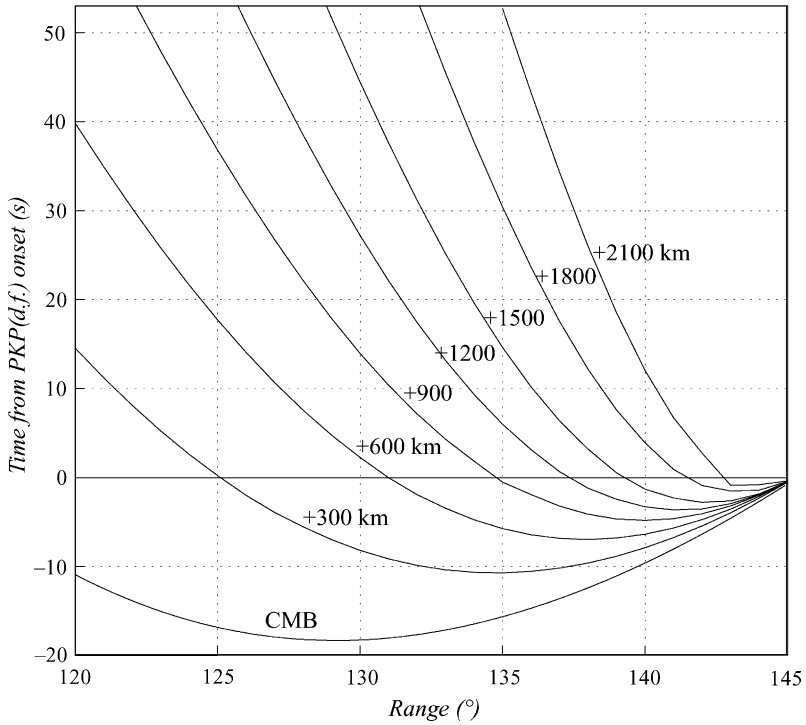

Fig. 2. Minimum travel time curves for energy scattered once in the mantle.The lowest curve indicates the minimum travel time of energy single-scattered at the CMB. The other curves represent the minimum travel time for scattering occurring at 300 km intervals up into the mantle, with the last curve representing scattering 2100 km above the CMB. These curves show that at short ranges and early times only scatterers close to the CMB can cause precursors, while at longer ranges and later times an increasing fraction of the mantle can contribute to the precursor wavetrain. While the precursor arrivals are prized due to lack of interference from other seismic waves, the preponderance of scattered waves in the mantle are predicted to arrive after PKP (df). The travel times were calculated using the PREM velocity model (Dziewonski and Anderson, 1981).

the primary sources of PKP coda and how they might be related to simple first-order models of mantle scattering. Limitations in the data coverage, and tradeoffs between the depth and the position of possible scattering sources, likely prevent resolution of more complicated three-dimensional structures that might also explain our observations. It should also be recognized that the models that we present here do not necessarily represent true spherical averages of mantle properties, due to the uneven sampling provided by the available PKP data.

2. Data

We have analyzed 3624 recordings of PKP precursors and coda that were made between day 151 of 1988 and the end of 1999 by stations in the Incorporated Research Institutions for Seismology (IRIS) Global Seismographic Network (GSN). These recordings were selected from a much larger dataset on the basis of pre-event noise levels. We rejected traces that exhibited noise levels that were high or varied sharply with time. To avoid bias toward high amplitude precursors, records were selected solely on the character of the noise, we did not consider the amplitude of the precursors. The events in the culled dataset occurred at depths from the near-surface to 657 km. About 60% of the events occurred within 100 km of the free-surface. The events were assigned body wave magnitudes between 5.0 and 7.3. Although, the GSN stations are distributed across the globe, the tight range limits on the recordings (120–145°) resulted in a rather uneven sampling of

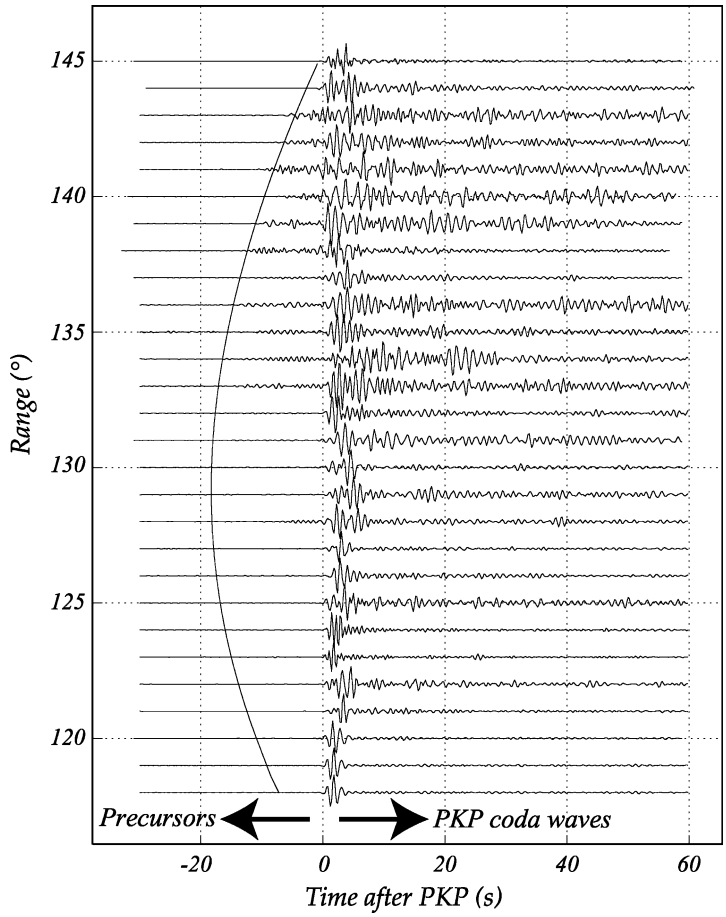

Fig. 3. Selected recordings of PKP precursors, main phase and coda made by stations in the IRIS–GSN between 118 and 145°. The data have been bandpassed between 0.7 and 2.5 Hz and are aligned on the PKP (df) onset. The traces reveal a gradual increase in the amplitude of the precursors and coda waves as a function of range. In this study we considered precursors within 20 s of PKP and coda within 60 s of the onset of PKP.

the Earth (Fig. 4). Some areas are not sampled at all.

3. Preliminary data analysis

The traces in Fig. 3 reveal a strong dependence of the precursors and coda waves on range and time. The precursors and coda increase in amplitude relative to PKP from 120 to 144°. Energetic coda is seen in most traces to 60 s after the arrival of PKP. The traces, however, also reveal variations that are clearly not global in origin but are regional. One notable example to this is the trace at ∼137° which is dominated by PKP. This trace implies weak scattering within the small volume of the mantle it samples. An earlier paper (Hedlin and Shearer, 2000) examined regional variations in scattering. Here, however, we focus on the global characteristics of the data and the depth extent of the scattering region. Although, the time and range dependence of the scattered wave amplitudes can be seen in individual recordings, it is necessary to stack the data to average out regional variations and reveal globally averaged characteristics of the heterogeneity that give rise to the scattered waves. For this purpose, we binned each recording into the appropriate 1° bin, after correcting for event depth. Each trace was filtered between 0.7 and 2.5 Hz and converted to an envelope. Prior to

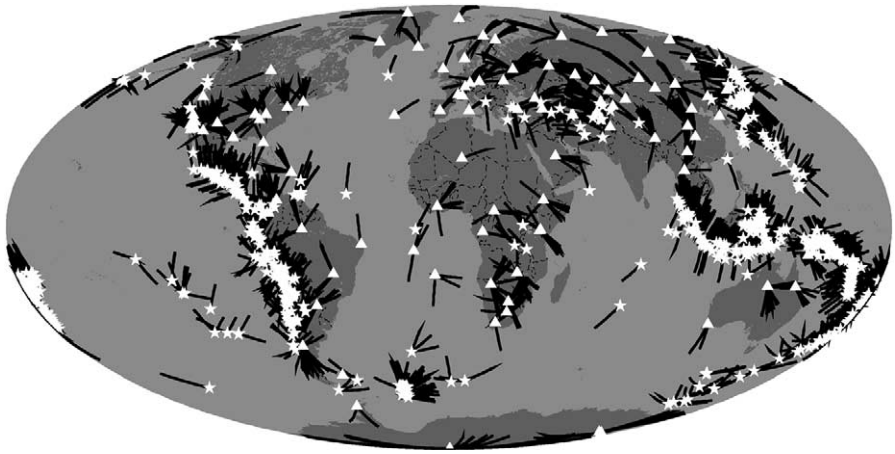

Fig. 4. In the figure, we plot sources, receivers and the path of PKP (df) in the mantle for records made between 130 and 141°. The sources and receivers are represented by stars and triangles, respectively. We see that even a relatively uniform global network such as the IRIS–GSN offers highly variable coverage. Some areas, such as near the seismically active regions in the southwest Pacific, are densely sampled while other regions (e.g. beneath the Atlantic and Indian oceans) are untouched. The global network coverage is limited largely because of the restricted range within which precursors can be observed. Any global study of PKP precursors must presently rely on a limited sampling of the mantle. A fuller description of the variability in the coverage of the mantle afforded by PKP data is given in Hedlin and Shearer (2000).

stacking, we applied a small, downward, adjustment of the amplitude to adjust for pre-event noise. The binning procedure grouped recordings simply on the basis of recording range and not on the location of either the source or the receiver. The stacked traces thus provide an image of the average characteristics of the arrivals.

The stacks shown in Figs. 5 and 6 indicate that coda amplitudes at ranges from 120 to 125° are nearly independent of range. No precursor energy is observed at these ranges. Between 125 and 144° we observe a gradual increase in the amplitude of the precursors and coda. The precursors at these ranges increase in amplitude from their onset to the PKP arrival. After PKP, the coda amplitudes decay gradually with time. Scattering simulations (Hedlin et al., 1997) indicate that most of the energy at ranges below 125° is due to near surface effects. Scattered wave amplitudes at these ranges are predicted to be low because the scattering volume is small and the incident waves are weak. PKP wave amplitudes increase in strength from 120° to the b caustic at 145°. A secondary effect is scattering directivity. The scattering angle becomes progressively larger with decreasing range and with increasing time. Small-scale scattering is directional with the strongest energy being associated with the smallest scattering angle. To illustrate the amount by which the amplitude of the precursors and coda increases from the low levels seen at ranges below 145°, we plotted a copy of the average stack from 120 to 125° at all ranges (see the dashed traces). This range dependence is unlikely due to near surface effects but we believe arises from scattering within the mantle. One notable exception is the bin centered at 136.5°. The amplitude of the scattered energy in this bin decreases prior to the arrival of PKP and remains low to the end of the window.

At 145°, the traces are dominated by PKP as the b caustic arrives at this range. All scattered waves are small in amplitude relative to PKP at these ranges and the relative amplitudes of the precursors and coda arrivals are comparable to those observed below 125°.

The suites of curves in Figs. 5 and 6 indicate the minimum travel time for single-scattered energy scattered at depths ranging from the CMB to 2200 km above. These figures illustrate the point that most scattered waves will follow, not precede, PKP. Fig. 6 also includes a histogram that shows the number of recordings used in each bin. We selected relatively

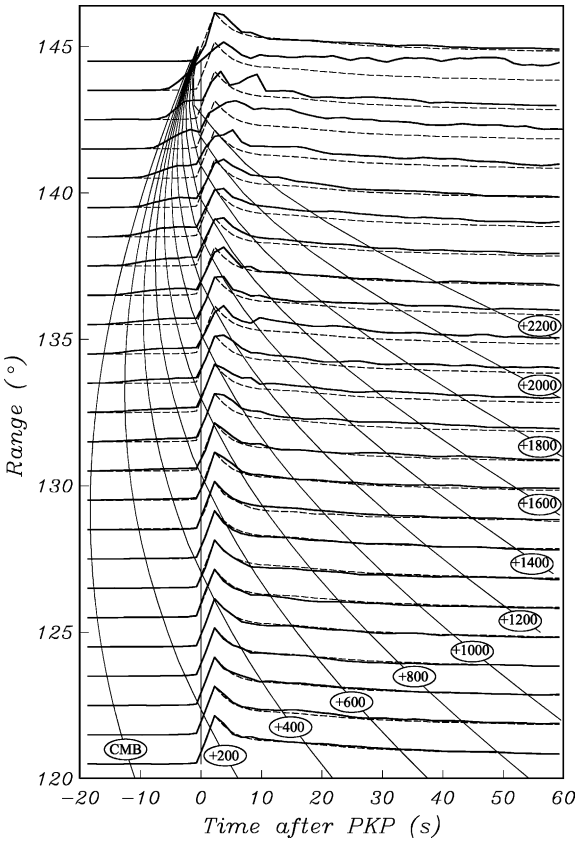

Fig. 5. Average precursor and coda amplitudes as a function of time and source–receiver range as obtained from a waveform stack of 3624 seismograms. Times are relative to the onset of PKP (df). Each stacked trace is normalized to the peak PKP (df) amplitude (at about 2 s). The theoretical onset time from the PREM velocity model for single-scattering at a range of depths from the CMB to 2200 km above the CMB are shown as the curved lines. Note the increase in precursor and coda amplitudes with range and the gradual decay of coda amplitudes with time. The dashed curve at each range represents the average stack between 120 and 125°.

few recordings near the b caustic because of the high-amplitude of precursors at these ranges and the resulting difficulty of accurately picking the onset of PKP.

4. The depth extent of mantle scattering

Hedlin et al. (1997) considered the factors listed in the previous section and modeled a stack of 1600 PKP precursor recordings using Rayleigh–Born scattering theory (Chernov, 1960) applied to the exponential autocorrelation function. The modeling indicated that the global average small-scale heterogeneity has a scale length of ∼8 km and is distributed uniformly throughout the lower-mantle with an rms velocity contrast of 1%. The adherence of the onset of precursors with the minimum travel time for scattering at the CMB (Figs. 5 and 6) precludes scattering within the outer core which would produce arrivals before the observed onset of the precursors (Shearer et al., 1998).

We are attempting to re-examine the vertical distribution of heterogeneity in the mantle using coda waves to check the earlier study. This requires careful consideration of the paths energy might take through the core before or after scattering in the mantle. As seen in the upper panel of Fig. 7, propagation through the mantle from the surface to the CMB involves no triplications. Propagation from the CMB back to the surface after propagation through the core is along one of four branches of PKP (Fig. 1). The earliest arriving branch at ranges between ∼119 and 132° is bc which represents prograde refraction through the outer core. The ab branch lags behind by a few seconds at most. The total travel time from the surface, to the scattering point and then back to the surface, is given by a sum of the two curves shown in Fig. 7. The curves show that the ab and bc branches alone can yield precursors to PKP. These branches were considered by Hedlin et al. (1997). The other branches can be associated only with coda arrivals. The df branch arrives first at ranges from 109 to ∼119° and beyond 132° and thus makes possible scattered coda arrivals across a greater range interval than is possible from either the ab or bc branches.

Precursors and coda to PKP are due to scattering from a small volume of the mantle near the source or the receiver. A hypothetical source considered in the two panels of Fig. 8 illustrates this point. In the figure, we show the locations on the CMB where scattering can occur on the source side of the path and produce scattered waves at the surface at a range of 135.5°. In the upper panel, we show the time lag between PKP and the single-scattered energy if we just consider propagation through the core along the ab and bc branches. The eastern limit of the colored patch is the curve along which the b caustic intersects the cmb.

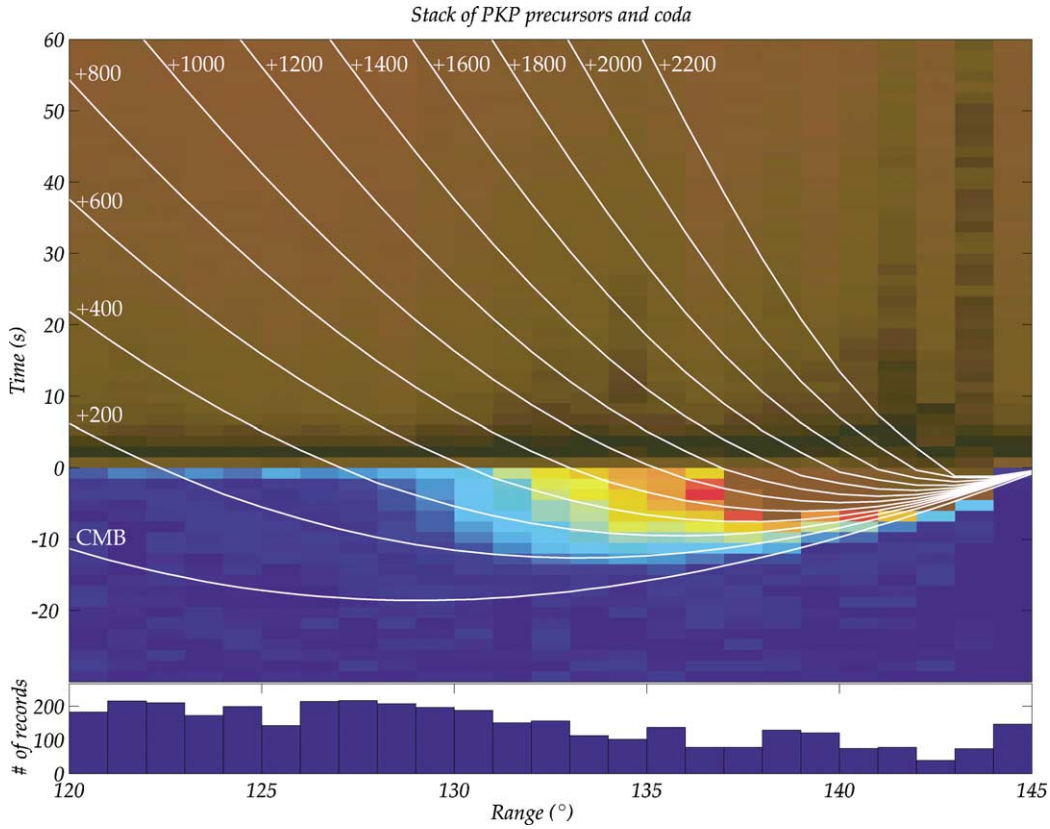

Fig. 6. The upper figure shows the average amplitude of PKP (df) and its precursors and coda at ranges between 120 and 145° resulting from a stack of 3624 short-period seismograms. Time is relative to the onset of PKP (df). The amplitude of the precursors increases gradually with increasing range and time. The precursors first appear at 124° and become indistinguishable from PKP (df) by 143°. The white curves show the minimum travel times for scattered waves at several depths in the mantle calculated using the PREM velocity model. Scattering that occurs at the CMB gives rise the earliest precursors. Scattering in the outer core can produce earlier arrivals but none are observed. The increase of coda amplitudes with increasing range is evident here. The lower panel shows the number of traces used in each 1° bin. Relatively few traces were selected beyond 142° because of the inherent difficulty in separating PKP from its energetic precursors.

This curve is highlighted in black. Outer core refracted waves beyond this curve are not possible. The western limit is due to the inner core. Outer core refracted waves cannot propagate beyond about 141° because waves that penetrate more deeply reflect from the inner core boundary and propagate to shorter ranges along the cd branch. Points that can give rise to precursors to PKP are located between the red curve and the b caustic. Later arrivals are expected from scattering points directly beneath the source and located off the great-circle path between the source and receiver.

If we consider energy that refracts through the inner core after scattering at the CMB, we must consider a much larger region on the CMB (lower panel). Inner core refracted scattered waves can originate at greater range from the source (beyond the b caustic) and at points further to the west of the source (Fig. 7). As mentioned earlier, the df branch cannot yield precursors and as a result, the region between the red curve and the b caustic is the same in the upper and lower panels of Fig. 8. We have chosen near-source scattering to illustrate sampling at the CMB. The grid of points near the receiver that gives rise to precursors and coda is the same.

The object of this paper is to determine if PKP coda will allow us to place a tight constraint on the

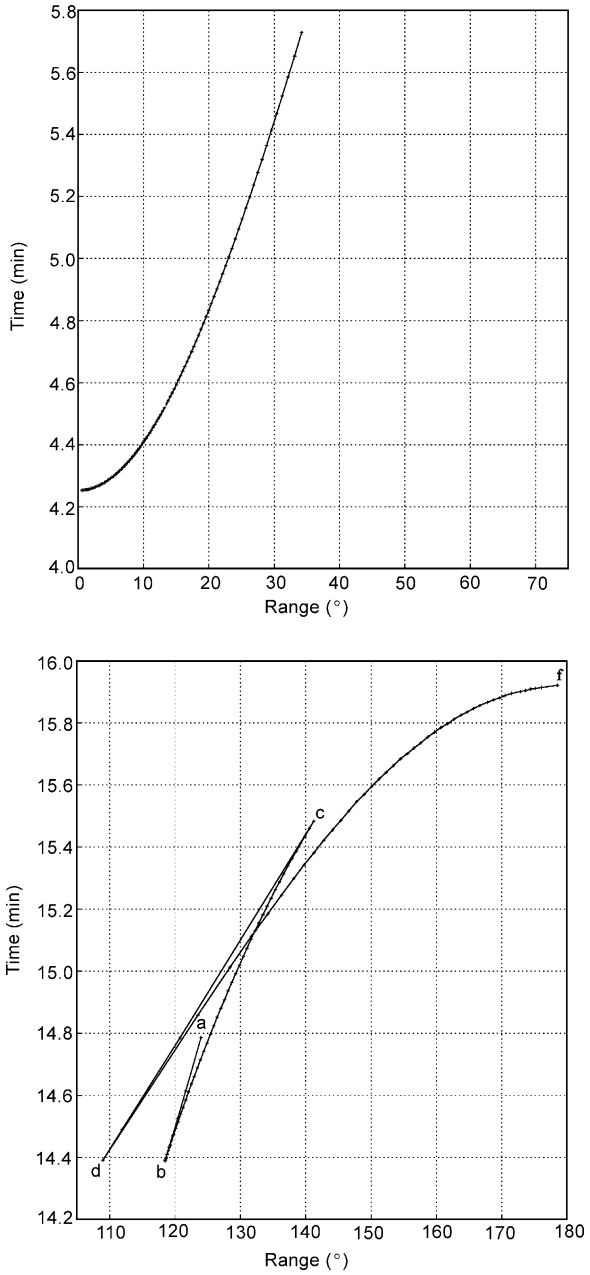

relative importance of scattering at shallow and great depths in the mantle. To investigate the vertical distribution of heterogeneity in the mantle we divide the mantle into thin (20 km) layers, from the CMB to the crust, and calculate the response of each individual layer to the incident wavefield. The statistics of the heterogeneity are invariant within each layer and are allowed to change only in strength between layers. The calculation used in this paper is identical to the single-scattering theory used by Hedlin et al. (1997). We assume that the mantle behaves like a Poisson solid and that the random perturbations in velocity have an exponential autocorrelation function (Wu and Aki, 1985). We neglect the influence of multiple scattering. The inner core attenuation model of Bhattacharyya et al. (1993) is used. One important difference from the earlier study is that we predict the amplitudes of PKP coda as well as precursors. As a result, we also consider d.f. refracted scattered waves. In Fig. 9, we show the scattering kernels for 12 of these layers ranging in depth from the CMB to 2200 km above. All scattering kernels were calculated assuming an exponential autocorrelation function with an 8 km scale-length and a source–receiver range of 135.5°. As observed by Hedlin et al. (1997), the earliest and largest contributions will come from the deepest layers and that, at this range, the precursors must originate from a volume within 1000 km of the CMB. Scattering that occurs at higher levels will produce arrivals after PKP (df) in the coda. The red curves represent the amplitude of scattered waves that propagate through the outer core along the ab or bc branch of PKP. If we include the df branch, we find that large contributions are expected beginning at PKP. The amplitude of the d.f. scattered arrivals decays with time but is largely independent of the depth of the heterogeneous layer. Although, this result is not shown, the amplitude of the d.f. refracted scattered waves is also largely independent of range.

By summing the energy of different combinations of these kernels we can explore the effect of scattering

Fig. 7. Travel time of P wave energy that propagates from the surface to a location on the CMB (top) and then back to the surface after propagating downward through the core (lower panel) assuming PREM (Dziewonski and Anderson, 1981). The total travel time through the earth of energy single scattered at the CMB is given by a sum of these two times. Energy propagates through the core along one of four branches as explained in Fig. 1. Scattered energy that propagaties along the ab or bc branch of PKP will arrive relatively early and might precede PKP. Any study of late-arriving scattered energy must consider all branches through the core, including the df branch which refracts through the inner core.

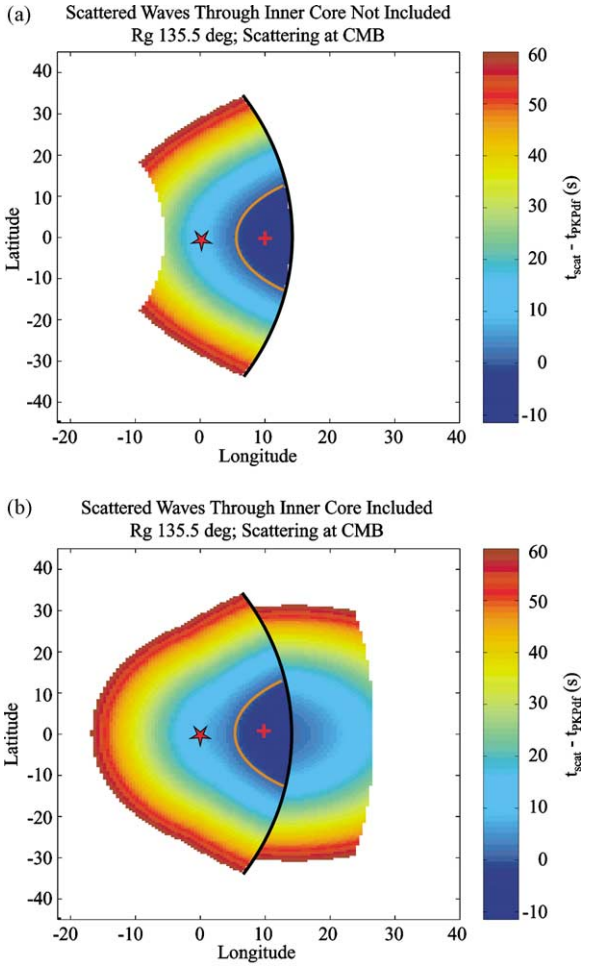

Fig. 8. The two plots show residual travel times for energy single-scattered from P to PKP at the CMB when compared with PKP (df) arrival times. In the figure, the receiver is located due east of the source (the five pointed star) at a range of 135.5°. (a) We allow scattered wave propagation through the outer core only. (b) It allows propagation through the inner core. At this range, the first arriving energy is expected 15.2 s before PKP (df) and is scattered from a point adjacent to the b caustic (marked by the black curved line) in the diametral plane of the source and receiver. On the conjugate side of the travel path there are equivalent contours which describe the isotimes associated with near-receiver scattering. The red curve on each plot above indicates the locations at which single-scattered energy will arrive at the same time as PKP (df). This curve envelopes the point at which PKP (df) enters the core (cross). Scattering at the CMB outside these patches will produce PKP coda. The area within which scattering can produce precursors and early coda arrivals becomes progressively smaller with decreasing depth. The calculation was based on the PREM global velocity model.

within different mantle depth intervals. The dashed curves in Fig. 9 are the predicted amplitudes of scattered waves assuming uniform 1% rms velocity perturbations at all depths (i.e. the curves were derived from an unweighted sum of all kernels). The dashed red curve corresponds to propagation through the core along the ab or bc branches alone. The dashed black curve includes these branches and the inner core df

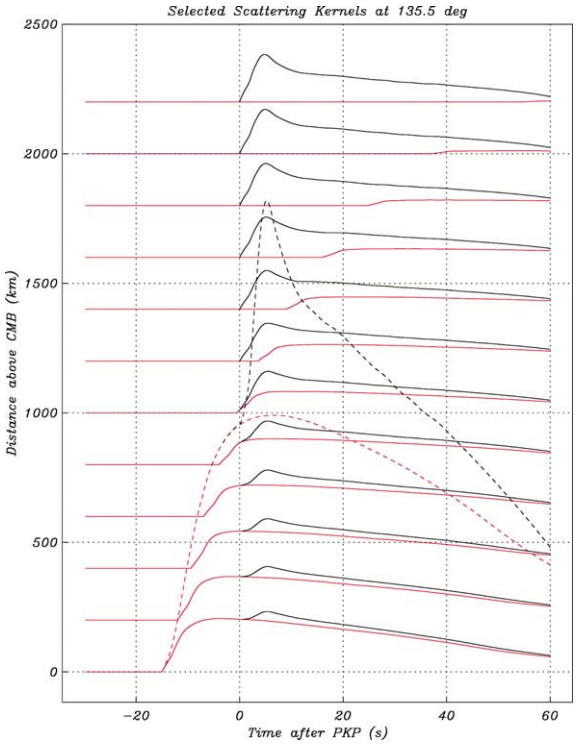

Fig. 9. Scattering energy kernels for random mantle velocity perturbations at selected depths from CMB to 2200 km above. The kernels were calculated assuming an exponential autocorrelation function with an 8 km scale and a source–receiver range of 135.5°, and have been convolved with an empirical source–time function derived from the PKP (df) arrivals in the stack. The energy in the source–time function is concentrated in the earliest 6 s but spans 60 s to include the coda arrivals. The red curves represent scattering wave amplitudes resulting from propagation of scattered waves through the outer core only (along the ab and bc branches of PKP). The black curves are the kernels that result from the calculation that also allows propagation along inner core branch df The square root of a sum of these energy kernels can be used to model recorded data amplitudes. The red dashed curve is the unweighted sum of all kernels that allow propagation through the outer core. The black dashed curve is the unweighted sum of the kernels that also allow propagation of scattered energy through the inner core.

branch. As all energy that propagates through the inner core is late, the two simulations are identical before PKP.

To model the data using these kernels it is necessary to take into account the ab, bc and df branches of PKP as well as late-arriving energy that results from scattering and resonance in the near-surface. We have observed that the coda amplitudes are independent of range when the recording is made at ranges below about 125°. The stacking procedure combines traces from widely separated regions of the Earth. The averaging of coda amplitudes removes regional variations and produces an estimate of the average near-surface energy levels we can expect at all ranges. The range independent average also includes energy that results from scattering in the mantle and propagation through the inner core along the df branch (Fig. 9). Our simulations indicate that the df branch has a weak dependence on range when compared with the ab and bc branches which are strongly influenced by the b caustic. The simulations also clearly show that regardless of what scattering model is used, the ab and bc branches produce essentially no scattered energy before or after PKP at ranges below 125°. To take into account and remove from consideration, near-surface effects and the inner core refracted scattered energy, we subtract the average coda amplitude observed at ranges below 125° from all bins. As shown in Fig. 10, the average stacked coda from 120 to 125° possesses minor variations with time. To ensure that this structure is not introduced into the stacks by the correction procedure, we approximate the average stack using a standard coda decay model (Pechmann et al., 2000). We assume the coda envelope amplitude as a function of time, $A(t)$, can be described as follows:

$$\log[A(t)] = \log[A_o] - \alpha \log(t - t_p)$$

where t_p is the time of the PKP onset, A_o the onset amplitude, α a free fitting parameter. We derived a best fit decay function (dashed curve in Fig. 10) which we deduct from the bins at all ranges. The correction applies only to the data points at times after the onset of PKP.

The result is given in Fig. 11 for the bins between 130 and 141°. The bins at greater ranges are difficult to interpret due to proximity to the b caustic. The bins

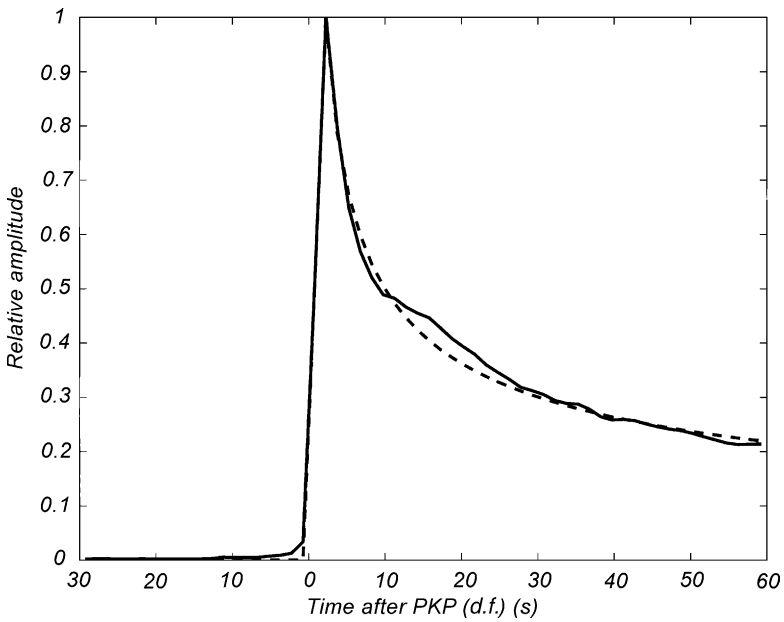

Fig. 10. The stack of all traces from 120 to 125° is shown by the solid black curve. The best fit curve, based on a standard coda decay model, is given by the dashed curve. We use this smooth function to correct coda amplitudes at ranges above 130°.

at ranges below 130° provide little insight as there is very little energy before PKP or after PKP once the correction for d.f. and the near-surface effects is made. At each range we show the stacked, and corrected, data and the standard errors from a resampling analysis. The standard errors increase after the arrival of PKP. This is expected as coda amplitudes are largely due to near surface effects. These effects depend on the depth of the event. Most events were located within 100 km of the surface, but some events were >600 km in depth. While we have observed robust range independent estimates of coda amplitudes at ranges below 125° and have inferred similar behavior at greater ranges, wide variability in the amplitudes that are present in individual traces is revealed by the resampling analysis (Efron and Tibshirani, 1991).

Despite the scatter in the corrected PKP coda amplitudes shown in Fig. 11, it is clear that the coda energy remains well above zero even after corrections for near-surface scattering are applied, implying that scattering from the CMB and/or deep mantle is a significant contributor to PKP coda energy at these ranges. This result could have been anticipated from Fig. 5, given the observed increase in PKP coda amplitude for those ranges where such deep scattering could occur. One goal of this paper is to test whether these PKP coda observations can place new constraints on the depth extent of lower mantle scattering.

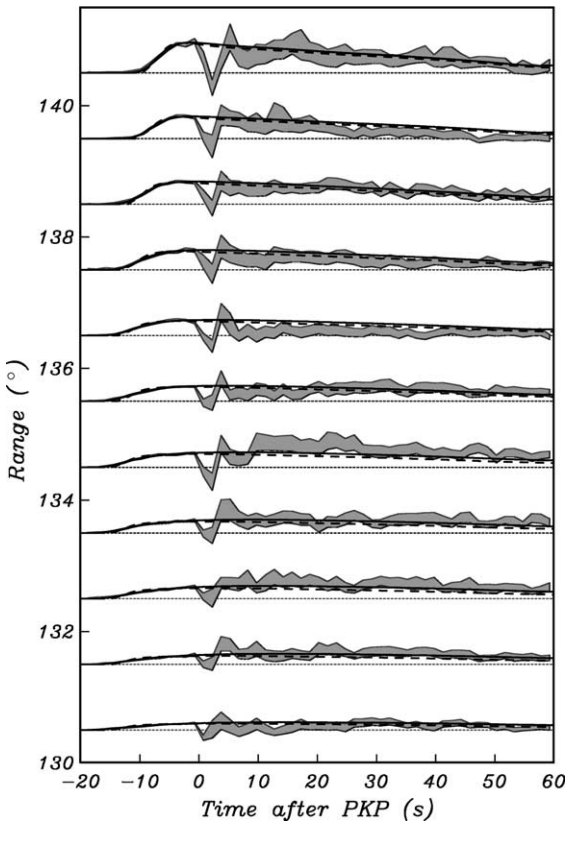

Fig. 11. Observed PKP (df) precursor and adjusted coda amplitudes compared to theoretical predictions of two models of mantle heterogeneity. The whole-mantle simulations are shown by the solid curve, the CMB only simulations are represented by the dashed curves. The data and their standard errors are indicated by the grey shaded regions. Coda decay is explained equally well by these two extreme models of mantle heterogeneity.

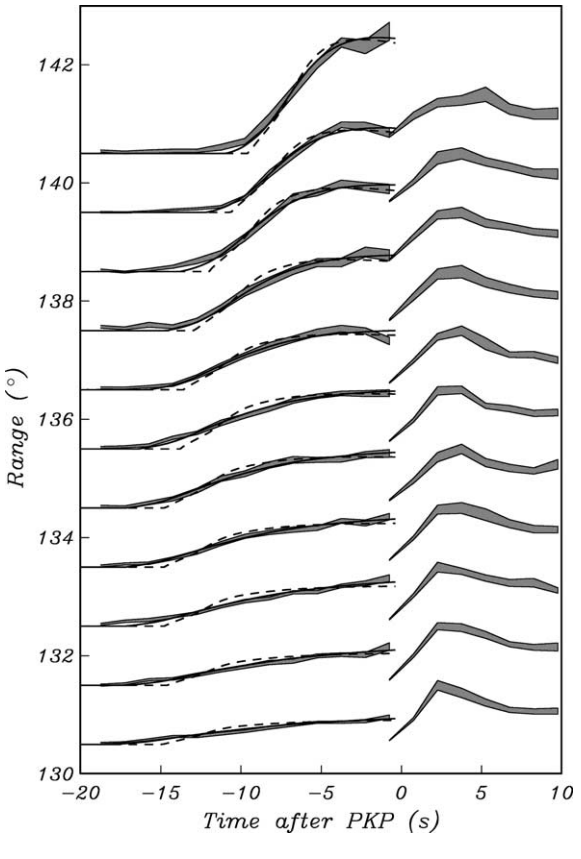

Fig. 12. Observed average PKP (df) precursor and coda amplitudes at ranges between 130.5 and 140.5° compared to theoretical predictions of two models of mantle heterogeneity. The data and their standard errors are indicated by the grey shaded regions. Only the whole-mantle model (solid) provides an adequate overall fit to the data. The model that allows heterogeneity just at the CMB requires onsets that are more rapid than those observed in the data.

Predicted results from two different models are shown in Fig. 11. One model (represented by the dashed curves) allows 8 km scale length heterogeneity within a 20 km-thick mantle layer immediately above the CMB and models the effect of scattering at or very close to the CMB (short-wavelength topography on the CMB would produce similar effects). The second model (solid curves) allows 8 km heterogeneity to be uniformly distributed throughout the mantle. For each model, we adjusted the rms amplitude of the velocity variations to obtain the best fit to the PKP precursors. Our simulations reveal that coda decay rates are nearly independent of the vertical distribution of heterogeneity in the mantle. The CMB-only model predicts slightly more rapid decay of coda amplitudes after PKP. This difference is seen at all ranges. Taking into account uncertainty about the coda amplitudes as determined from a resampling analysis, our stacks indicate that both models are in nearly equal agreement with the data. Both predict an increase in energy before PKP and then a gradual decay.

However, as noted in Hedlin et al. (1997), the two models do not produce equal fits to the PKP precursors. Fig. 12 presents a closer view of the precursors

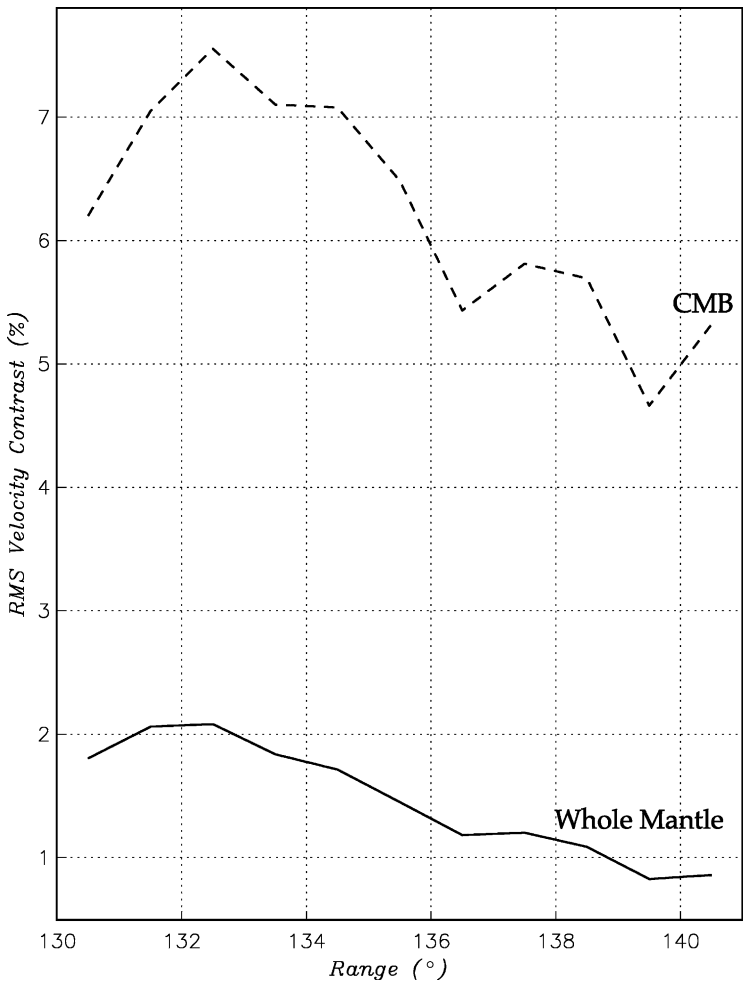

Fig. 13. The rms velocity contrasts required by two extreme models of mantle heterogeneity are shown above. The “whole mantle” model allows 8 km scale heterogeneity distributed uniformly through the mantle. The “CMB” model restricts 8 km scale heterogeneity to the lowermost 20 km of the mantle (to serve as a proxy for CMB topography).

and the model fits before PKP. Our analysis of 3624 recordings validates the conclusions of Hedlin et al. (1997) which were based on a much smaller dataset (∼1600 traces). The model that allows small-scale heterogeneity to be distributed uniformly throughout the mantle provides the only adequate fits to the data. The model that includes heterogeneity just at the CMB produces onsets that are more rapid than observed. In addition, the CMB scattering model requires much larger velocity perturbations to achieve the same amplitude of scattering. The whole mantle model requires rms velocity perturbations between 1 and 2% whereas the CMB scattering model requires perturbations of 5.5–7.5% within the deepest 20 km of the mantle (Fig. 13).

5. Conclusions

Our analysis of 3624 teleseismic recordings of PKP precursors and coda indicates that coda arrivals do not provide a useful constraint on the vertical distribution of heterogeneity within the mantle. There are two reasons for this. While the onset of scattered energy depends strongly on the vertical distribution of heterogeneity, the coda decay rates are nearly insensitive to this. The second reason is that the statistical variability of coda amplitudes is high. The standard errors of the stacked data are greater than the difference between the coda amplitudes predicted by the two models.

Our analysis of simulated and recorded data indicates that PKP precursors remain the most effective probe of small-scale heterogeneity in the mantle. Specifically, the increase in the amplitude of the precursors with time and increasing range appears to be a diagnostic indicator of the vertical distribution of the heterogeneity. Our analysis of 3624 high-quality teleseismic recordings confirms the conclusions of Hedlin et al. (1997). PKP precursors are consistent with scattering uniformly distributed throughout the lower mantle and not with scattering confined to the CMB. The preferred model requires ∼1% rms heterogeneity with a scale length of 8 km at all depths. In our analysis we assumed Rayleigh–Born scattering and an exponential autocorrelation function. Tests with a gaussian autocorrelation function produced essentially the same results. The data used in this study were bandpassed between 0.7 and 2.5 Hz. Further study using different pass bands will be required before conclusions can be drawn about the nature of mantle heterogeneity at different scale lengths.

The binning procedure used in this paper did not take into account the depth of the event, just the range. Event depth was used only to increase the range of the recording slightly to place the source back at the surface. The adjustment was necessary as all simulations assumed the source was located at the free-surface. As the global networks collect more teleseismic recordings it will eventually be possible to achieve robust estimates of PKP precursors and coda by using stacks of recordings binned by source–receiver range and by depth. Much of the variability of coda amplitudes is due to differences in event depth. Shallow events typically produce the most energetic coda. Binning by depth would remove this source of variability in coda amplitudes and reduce the standard errors seen in the stacks. Tighter bounds on coda amplitudes might make it possible to differentiate between scattering models that have heterogeneity located at different depth intervals in the mantle.

The present study relied on vertical component recordings of the scattered waves made by widely separated stations in the GSN. It might be possible to place tighter bounds on the location of scattering in the mantle by analysis of array data (provided by deployments including the large-aperture Norwegian seismic array (NORSAR), the large-aperture American seismic array (LASA) or numerous deployments in the IRIS PASSCAL program). Additional constraints on particle motion and thus the origin point of the scattered waves might be provided by three-component data. This study considered data filtered in time between 0.7 and 2.5 Hz. Scattering occurs at a broad range of scales in the mantle but narrow band filtering of broadband data restricts our view of mantle scattering to a narrow range of spatial scales. The bandpass filtered data are best fit by a mantle model that includes 8 km scale length heterogeneity. Analysis of the entire spectrum of seismic energy might reveal more completely the nature of the heterogeneous mantle.

Vidale and Earle (2000) found evidence for weak scattering in the inner core by examining LASA recordings of faint coda to PKP (cd) at ranges between 58 and 73° from the source. At this time, it is

not known how strong and how dependent on time and range, inner core scattered waves might be beyond 125°. The question of how significant inner core scattered waves are relative to mantle scattered waves is an important issue that we hope to address in future work.

Acknowledgements

This research was made possible by high-quality data in the FARM archive at the IRIS DMC. This research was funded by National Science Foundation EAR99-093370.

References

Bataille, K., Flatté, S.M., 1988. Inhomogeneities near the core-mantle boundary inferred from short-period scattered PKP waves recorded at the global digital seismograph network. J. Geophys. Res. 93, 15057–15064.

Bhattacharyya, J., Shearer, P.M., Masters, G., 1993. Inner core attenuation from short-period PKP (BC) versus PKP (df) waveforms. Geophys. J. Int. 114, 1–11.

Chernov, L.A., Wave Propagation in a Random Medium (R.A. Silverman, Trans.). McGraw-Hill, New York, 1960.

Cleary, J.R., Haddon, R.A.W., 1972. Seismic wave scattering near the core-mantle boundary: a new interpretation of precursors to PKP. Nature 240, 549–551.

Doornbos, D.J., 1976. Characteristics of lower mantle inhomogeneities from scattered waves. Geophys. J. R. Astronom. Soc. 49, 541–542.

Cormier, V., 1995. Time domain modeling of PKIKP precursors for constraints on the heterogeneity in the lowermost mantle. Geophys. J. Int. 121, 725–736.

Doornbos, D.J., 1978. On seismic-wave scattering by a rough core-mantle boundary. Geophys. J. R. Astronom. Soc. 53, 643–662.

Doornbos, D.J., Husebye, E.S., 1972. Array analysis of PKP phases and their precursors. Phys. Earth Planet. Interior 5, 387.

Dziewonski, A., Anderson, A.M., 1981. Preliminary reference Earth model. Phys. Earth Planet. Interior 25, 297–356.

Efron, B., Tibshirani, R., 1991. Statistical data analysis in the computer age. Science 253, 390–395.

Haddon, R.A.W., 1972. Corrugations on the CMB or transition layers between inner and outer cores? Trans. Am. Geophys. Union 53, 600.

Haddon, R.A.W., Cleary, J.R., 1974. Evidence for scattering of seismic PKP waves near the mantle-core boundary. Phys. Earth Planet. Interior 8, 211–234.

Hedlin, M.A.H., Shearer, P.M., Earle, P.S., 1995. Imaging CMB scatterers through migration of GSN PKP (df) precursor recordings. EOS 76, F402.

Hedlin, M.A.H., Shearer, P.M., Earle, P.S., 1997. Seismic evidence for small-scale heterogeneity throughout the Earth's mantle. Nature 387, 145–150.

Hedlin, M.A.H., Shearer, P.M., 2000. An analysis of large-scale variations in small-scale mantle heterogeneity using Global Seismographic Network recordings of precursors to PKP. J. Geophys. Res. 105, 13655–13673.

Husebye, E.S., King, D.W., Haddon, R.A.W., 1976. Precursors to PKIKP and seismic wave scattering near the mantle-core boundary. J. Geophys. Res. 81, 1870–1882.

King, D.W., Haddon, R.A.W., Cleary, J.R., 1974. Array analysis of precursors to PKIKP in the distance range 128–142°. Geophy. J. R. Astronom. Soc. 37, 157–173.

Pechmann, J.C., Nava, S.J., Bernier, J.C., Arabasz, W.J., 2000. A critical analysis of systematic time-dependent coda-magnitude errors in the university of utah earthquake catalog, 1981–1999. EOS 81, F869.

Shearer, P.M., Hedlin, M.A.H., Earle, P.S., 1998. PKP and PKKP precursor observations: implications for the small-scale structure of the deep mantle and core. Geodynamics 28, 37–55.

Vidale, J.E., Earle, P.S., 2000. Fine-scale heterogeneity in the Earth's inner core. Nature 404, 273–275.

Vidale, J.E., Hedlin, M.A.H., 1998. Evidence for partial melt at the core-mantle boundary north of Tonga from the strong scattering of seismic waves. Nature 391, 682–685.

Wen, L., 2000. Intense seismic scattering near the Earth's core-mantle boundary beneath the Comoros hotspot. Geophys. Res. Lett. 27, 3627–3630.

Wu, R.S., Aki, K., 1985. Elastic wave scattering by a random medium and the small-scale inhomogeneities in the lithosphere. J. Geophys. Res. 90, 10261–10273.